Discrete Oligomers and Polymers of Chloride Monohydrate can form in Encapsulated Environments: Structures and Infrared Spectra of $[Cl_4(H_2O)_4]^{4-}$ and $\{[Cl(H_2O)]^-\}_\infty$

Rathiga Senthooran,[a] Owen J. Curnow,*[a] and Deborah L. Crittenden*[a]

Abstract: A discrete tetrachloride tetrahydrate cluster, $[Cl_4(H_2O)_4]^{4-}$, which is a tetramer of chloride monohydrate $[Cl(H_2O)]^-$, was obtained as a salt of (bis(2,2,2-trifluoroethyl)amino)(diethylamino)-(dipropylamino)cyclopropenium, $[C_3(N(CH_2CF_3)_2)(NEt_2)(NPr_2)]^+$. The cluster consists of a $[Cl_2(H_2O)_2]^{2-}$ square with each chloride coordinated by a water that is bridging to another chloride. A polymer of chloride monohydrate, $\{[Cl(H_2O)]^-\}_\infty$, was obtained with the cation $[C_3(N(CH_2CF_3)_2)_2(NBuMe)]^+$. This salt consists of a 1D chain of alternating Cl^- and H_2O bridges. Both salts were characterized by single-crystal X-ray diffraction and infrared spectroscopy. Infrared spectra were also collected on the D_2O isotopomers. Unlike the monomer and dimer of chloride monohydrate, both the tetrameric and polymeric structures were found to be computationally-unstable in the gas phase. This indicates that an encapsulated environment is essential for the isolation of these species. DFT and DFTB calculations were carried out on gas-phase $[Cl_4(H_2O)_4]^{4-}$ to assist the infrared band assignments. Anharmonically-corrected B3LYP transition frequencies were in close agreement with experiment but DFTB models were only appropriate for qualitative interpretation. The polymer was unstable in the gas phase, but solid-state DFTB calculations allowed the character of the vibrational modes to be elucidated and assigned. The spectroscopic and computational results are consistent with “discrete” chloride hydrate species.

Introduction

Monochloride monohydrate, $[Cl(H_2O)]^-$, is the simplest example of one of the more ubiquitous and important classes of anion solvates. Remarkably, there has been only one study of a discrete $[Cl(H_2O)]^-$ anion solvate in the solid state (Figure 1a),[1] although it has been characterized in the gas phase using infrared spectroscopy and its structure and vibrational spectrum have been the subject of intensive computational investigation.[2,3] Two other structures containing chloride monohydrates have also been reported, but there were no spectroscopic studies carried out as they were not recognized as such at the time.[4–6]

[a] Rathiga Senthooran, A/Prof. Owen J. Curnow
and A/Prof. Deborah L. Crittenden
School of Physical and Chemical Sciences
University of Canterbury, Private Bag 4800, Christchurch,
New Zealand
E-mail: owen.curnow@canterbury.ac.nz
deborah.crittenden@canterbury.ac.nz

Supporting information for this article is given via a link at the end of the document.

More commonly, chloride monohydrate is found in the solid state as its dimer dichloride dihydrate, $[Cl_2(H_2O)_2]^{2-}$ (Figure 1b), which has been calculated to be metastable in the gas phase.[7,8] We have recently reported three discrete examples of this dimer, each with different crystallographic symmetry (D_{2h}, C_{2h} and C_{2v}).[9] In each case, we used triaminocyclopropenium (TAC) cations as the counterion as they are known to have weak cation-anion interactions.[10,11] Five other examples of the dimer, all with C_{2h} symmetry, were already known, of which two could be considered discrete,[12,13] while the other three have significant NH–Cl^- and NH–OH_2 hydrogen bonding.[14–16]

We have also reported three other discrete dichloride hydrates: the monohydrate $[Cl_2(H_2O)]^{2-}$, the tetrahydrate $[Cl_2(H_2O)_4]^{2-}$, and the hexahydrate $[Cl_2(H_2O)_6]^{2-}$ (Figures 1c–e, respectively).[17–19] The monohydrate is not predicted to be stable in the gas phase (the hydrogen bonds are unable to make up for the electrostatic repulsion between the chloride ions),[4,8] whereas dichloride hydrates with at least three waters are predicted to be stable in the gas phase according to *ab initio* quantum chemical calculations.[4,7,8,20]

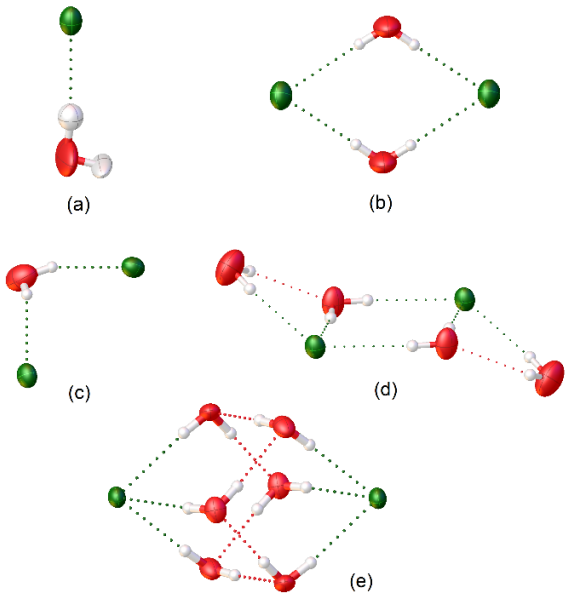

Figure 1. The structures of known discrete chloride hydrates (a) $[Cl(H_2O)]^-$; (b) $[Cl_2(H_2O)_2]^{2-}$; (c) $[Cl_2(H_2O)]^{2-}$; (d) $[Cl_2(H_2O)_4]^{2-}$; (e) $[Cl_2(H_2O)_6]^{2-}$.[1,9,17–19]

In terms of multi-chloride hydrate clusters, as distinct from polymeric chloride hydrates, Jian claimed a discrete $[Cl_6(H_2O)_8]^{6-}$ cluster in which the chloride ions are ligands on Cu complexes, and so we would not consider this to be discrete.[21] Notably, Seth described an almost identical compound that they described as containing a discrete $(H_2O)_8$ cluster.[22] Wang and Liu similarly claimed a discrete $[Cl_8(H_2O)_{10}]^{8-}$ cluster which in fact is a network with extensive hydrogen bonding to Cu-aquo ligands and NH substituents.[23] Thus, to our knowledge, there do not appear to be any discrete multi-chloride hydrate complexes. However, we are aware of several polymeric networks in which there are no strong interactions with the cations. Most of these are 2D networks, none of which have a 1:1 chloride:water ratio.[24] There are also four examples of 1D chains, three with a 1:2 chloride:water ratio and one with a 2:3 ratio.[25,26]

To further confirm the discreteness of encapsulated chloride hydrates, vibrational spectroscopy can be used to probe how bond strengths change due to interactions with the surrounding crystalline environment. If discrete, chloride hydrate bands within solid state IR spectra should closely match those predicted or observed[3] in the gas phase. However, vibrational modes associated only with chloride hydrates can be hard to pinpoint due to the presence of overlapping bands from other species present (e.g. OH and/or NH stretching modes). We have recently reported infrared and far-infrared band centres for several discrete chloride hydrate species encapsulated within cyclopropenium salts, using a selective deuteration strategy to clearly and uniquely identify the relevant vibrational transitions. [1,9,17–19]

In this work we present a structural and spectroscopic characterization of a discrete tetramer and a polymer of $[Cl(H_2O)]^-$, which represent the first discrete multi-chloride hydrate and first discrete polymer of $[Cl(H_2O)]^-$, respectively.

Results and Discussion

Synthesis

We have recently been investigating the synthesis and properties of partially-fluorinated TAC salts. We have previously reported that treatment of tetrachlorocyclopropene with $NH(CH_2CF_3)_2$ and NBu_3 leads primarily to a mixture of $[C_3(N(CH_2CF_3)_2)_2(NBu_2)]Cl$ and $[C_3(N(CH_2CF_3)_2)(NBu_2)Cl]Cl$, and that the latter can be further treated with the secondary amine $NHBu_2$ to give $[C_3(N(CH_2CF_3)_2)(NBu_2)_2]Cl$.[9] By using the less bulky tertiary amine NEt_3 instead of NBu_3, a small amount of the diaminochloro-TAC cation $[C_3(N(CH_2CF_3)_2)(NEt_2)Cl]^+$ is produced (Scheme 1). Addition of dipropylamine then gives a TAC salt with three different amino groups, namely $[C_3(N(CH_2CF_3)_2)(NEt_2)(NPr_2)]Cl$, which was crystallised as a monohydrate (**1**.H_2O). With the reaction using NBu_3, we have found that under shorter reaction conditions $[C_3(N(CH_2CF_3)_2)_2Cl]^+$ is formed in low yield and that addition of the secondary amine NHBuMe gives the C_s-symmetric cation $[C_3(N(CH_2CF_3)_2)_2(NBuMe)]^+$. This was isolated as the chloride salt and then also crystallised as the monohydrate $[C_3(N(CH_2CF_3)_2)_2(NBuMe)]Cl.H_2O$ (**2**.H_2O).

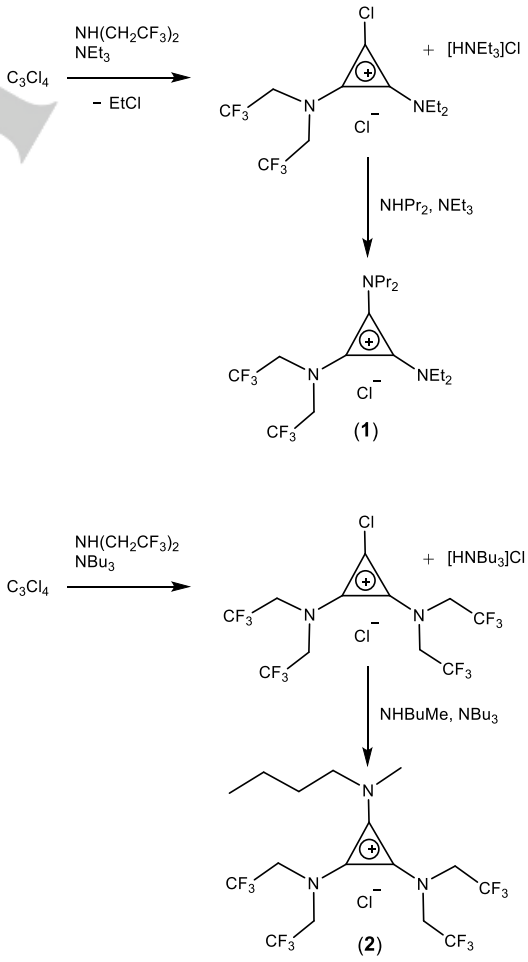

Scheme 1. Syntheses of $[C_3(N(CH_2CF_3)_2)(NEt_2)(NPr_2)]Cl$ (**1**) and $[C_3(N(CH_2CF_3)_2)_2(NBuMe)]Cl$ (**2**).

Table 1. Structure refinement data for $[C_3(N(CH_2CF_3)_2)(NEt_2)(NPr_2)]Cl.H_2O$ (**1**.H_2O) and $[C_3(N(CH_2CF_3)_2)_2(NBuMe)]Cl.H_2O$ (**2**.H_2O).

	1.H_2O	**2**.H_2O
formula	$C_{17}H_{30}ClF_6N_3O$	$C_{16}H_{22}ClF_{12}N_3O$
a [Å]	10.5845(4)	20.0175(8)
b [Å]	13.1134(5)	13.5771(5)
c [Å]	16.8299(6)	17.3399(6)
α [°]	81.231(3)	90
β [°]	78.237(3)	104.869(4)
γ [°]	79.347(3)	90
V [Å^3]	2231.45(15)	4554.8(3)
Z	4	8
ρ_{calc} [g cm^{-3}]	1.315	1.563
crystal system	triclinic	monoclinic
space group	*P*-1	$P2_1/c$
shape/colour	colourless	colourless
crystal size [mm]	0.285 × 0.214 × 0.151	0.275 × 0.121 × 0.059
μ [mm^{-1}]	0.232	0.278
T [K]	119.9(2)	120.0(3)
F(000)	928	2176
2*θ* range [°]	6.87 – 61.772	6.852 – 61.502
index ranges	$-14 \le h \le 14$	$-27 \le h \le 27$
	$-18 \le k \le 17$	$-16 \le k \le 19$
	$-23 \le l \le 24$	$-24 \le l \le 22$
reflections collected	60886	28446
independent reflns	12565	12061
R(int)	0.0329	0.0439
data/restraints/parameters	12565/0/529	12061/0/725
GoF on F^2	1.042	1.022
R_1/wR_2 [$I>2\sigma(I)$]	0.0523/0.1372	0.0587/0.1310
R_1/wR_2 (all data)	0.0675/0.1486	0.1018/0.1559
$\Delta\rho_{max/min}$/e [Å^{-3}]	0.95/–0.40	0.93/–0.50

X-ray crystallography

$[C_3(N(CH_2CF_3)_2)(NEt_2)(NPr_2)]Cl{\cdot}H_2O$ (**1**.H_2O) crystallizes in the triclinic space group *P*–1 (Table 1) in which the asymmetric unit consists of two cations, two chlorides and two waters (Figure 2). In each cation, all of the substituents except for one are on the same side; oriented away from the chloride hydrate so as to maximize CH–Cl$^-$ interactions involving methylene groups adjacent to the amine centres. Due to the reduced π donation from the fluorinated substituents, the exocyclic C–N bonds through which they are attached to the cyclopropenium ring are longer than observed for their non-fluorinated equivalents, by about 0.035 Å. The amine centres for the fluorinated substituents are also slightly non-planar; the sum of angles at N deviate from 360 by approximately five degrees. Atomic-labeling schemes and precise structural parameters for the cations are given in the Supporting Information.

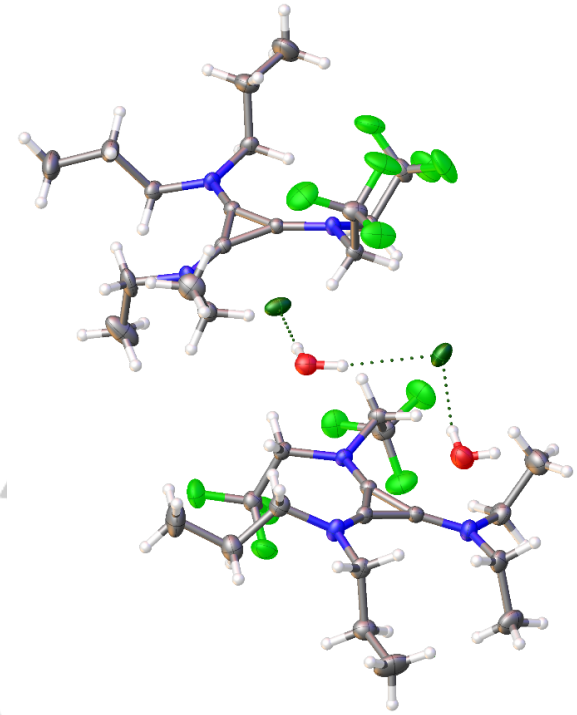

Figure 2. The asymmetric unit in **1**.H_2O.

The chloride hydrate forms a C_i-symmetric tetrameric structure of $[Cl_4(H_2O)_4]^{4-}$ which can be described as having a square $[Cl_2(H_2O)_2]^{2-}$ core with two additional terminal chloride monohydrates hydrogen bonding to the central chlorides (Figure 3). Structural parameters are given in Table 2. As such, it is structurally related to previously characterized discrete dichloride dihydrates (Figure 1b) and chloride monohydrate (Figure 1a). Alternatively, it may be thought of as a dichloride tetrahydrate (Figure 1d) with two additional terminal chloride ions that reorient the terminal water molecules into the plane of the Cl_2O_2 square, almost directly opposite one of the bridging waters (O-C-O angle of ~178°). Interestingly, however, the terminal chloride ions are not in the same plane (O-Cl-O-Cl dihedral of ~157°), presumably due to crystal packing effects.

Table 2. X-ray structural parameters for the chloride hydrate clusters in **1**.H_2O and **2**.H_2O.

1.H_2O		**2**.H_2O	
Parameter	X-ray	Parameter	X-ray
O1---Cl1 [Å]	3.2370(17)	O1---Cl1 [Å]	3.182(2)
O1'---Cl1 [Å]	3.3132(18)	O1---Cl2 [Å]	3.146(3)
O2---Cl1 [Å]	3.2062(16)	O2---Cl1 [Å]	3.134(3)
O2---Cl2 [Å]	3.1944(15)	O2---Cl2 [Å]	3.123(2)
Cl1---Cl2 [Å]	4.8805(7)	Cl1---Cl2 [Å]	4.6343(10)
Cl1---Cl1' [Å]	4.7906(10)	Cl1---Cl2' [Å]	5.1413(10)
O1---O2 [Å]	4.744(2)	O1---O2 [Å]	4.371(4)
O1---O1' [Å]	4.468(3)	O1---O2' [Å]	4.342(4)
Cl1–O2–Cl2 [°]	99.37(5)	Cl1–O1–Cl2 [°]	94.17(6)
Cl1–O1–Cl1' [°]	94.00(4)	Cl1–O2–Cl2 [°]	110.5(6)
O1–Cl1–O1'	86.00(4)	O1–Cl1–O2 [°]	86.86(6)
O1-Cl1-O2 [°]	94.84(4)	O1–Cl2–O2 [°]	88.42(6)
O1'–Cl1–O2 [°]	177.85(4)	O1-Cl2-O2-Cl1	–115.70(5)

Cl1'-O1-Cl1-O2	178.01(4)	Cl2-O2-Cl1-O1	–126.05(8)
O1-Cl1-O2-Cl2	157.12(4)	O2-Cl1-O1-Cl2	169.60(5)
		Cl1-O1-Cl2-O2	157.33(6)

Compared to all previously characterized structures containing the dichloride dihydrate core and/or bridged chloride hydrates, our tetrachloride tetrahydrate more closely resembles the dichloride tetrahydrate in terms of Cl-O distances, as summarized in Table 3. The very weak water-water hydrogen bond within the dichloride tetrahydrate helps account for the strong structural similarities between these species.

Table 3. Comparison of Cl-O distances within dichloride tetrahydrate[18] and tetrachloride tetrahydrate clusters.

	$[Cl_2(H_2O)_4]^{2-}$	$[Cl_4(H_2O)_4]^{4-}$
Within core	3.2250(17) Å	3.2370(17) Å
Outside core	3.191(2) Å	3.2062(16) Å
Terminal	3.2900(16) Å	3.3132(18) Å

Another relevant structure is the dichloride monohydrate $[Cl_2(H_2O)]^{2-}$ which has one water bridging two chlorides, similar to the terminal chloride hydrate motif within $[Cl_4(H_2O)_4]^{4-}$. Structural comparisons are presented in Table 4. In both cases, these relatively exposed chlorides have a number of non-classical hydrogen bonds to CH_2 groups of the cations: for the terminal chloride in **1**.H_2O, there are five CH---Cl distances between 2.6–2.9 Å whereas the chloride within the square core has only two.

Table 4. Comparison of structural parameters for dichloride monohydrate[19] and tetrachloride tetrahydrate clusters.

	$[Cl_2(H_2O)]^{2-}$	$[Cl_4(H_2O)_4]^{4-}$
Cl-O distance	3.230(4) Å	3.2062(16) Å
Cl-O distance	3.215(4) Å	3.1944(15) Å
O-Cl-O angle	107.22(10)°	99.37(5)°

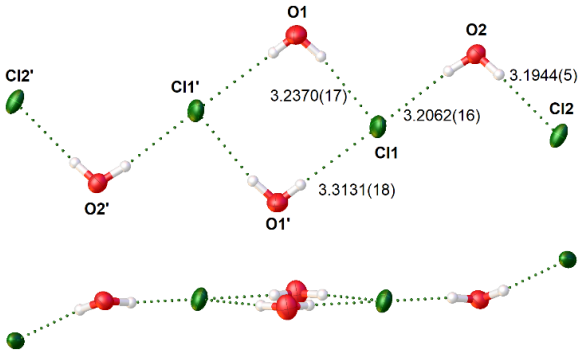

Figure 3. Top and side view of the C_i-symmetric tetrachloride tetrahydrate in **1**.H_2O (distances in Å).

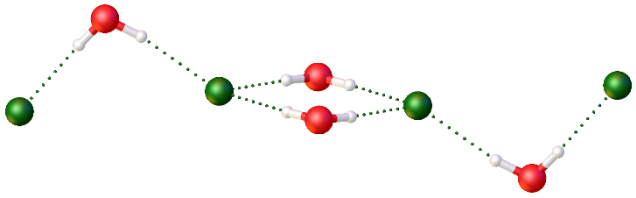

Figure 4. Calculated structure of $[Cl_4(H_2O)_4]^{4-}$ with fixed Cl atom positions performed at B3LYP/6-31+G(d,p).

The strong structural similarities of $[Cl_4(H_2O)_4]^{4-}$ with $[Cl_2(H_2O)_4]^{2-}$ and $[Cl_2(H_2O)]^{2-}$ support the idea that this is a discrete cluster with relatively weak interactions with the surrounding cations. Nonetheless, it is reasonable to assume that the near planarity of the system is probably a consequence of crystal packing as the external O-Cl-O angles are expected to be very soft. Indeed, a calculated structure (Figure 4) with fixed chloride positions results in outer waters that are out of the square plane and on opposite sides.

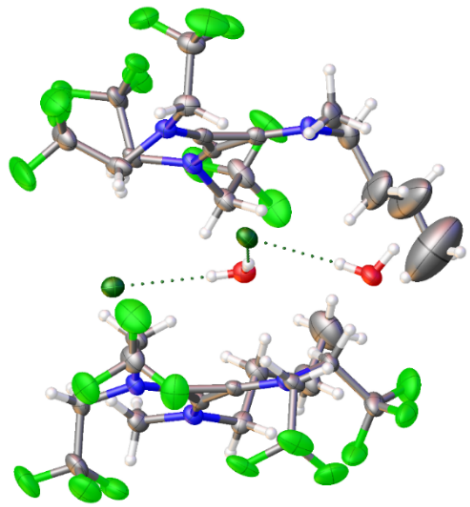

Figure 5. The asymmetric unit in **2**.H_2O.

$[C_3(N(CH_2CF_3)_2)_2(NBuMe)]Cl{\cdot}H_2O$ (**2**.H_2O) crystallizes in the monoclinic space group *P*21/*c* (Table 1). Like **1**.H_2O, the asymmetric unit also consists of two cations, two chlorides and two waters (Figure 5). Again, due to the reduced π donation from the fluorinated substituents, the corresponding exocyclic C–N bonds are longer than in the dialkylamino case (1.346 Å average versus 1.308 Å, respectively). In this case, the amino groups with fluorinated substituents are either planar but rotated with respect to the cyclopropenium plane, or they are non-planar. Further details are available in the Supporting Information.

The chloride hydrate forms a polymeric structure of alternating chlorides and waters within hydrophilic channels. The exterior consists of the fluorinated groups. Figure 6a shows the arrangement of the channels and Figure 6b illustrates the intermolecular interactions between the cations and the polymer chain. Structural details of these intermolecular interactions are provided in the Supporting Information (Table 5S). Each alternating chloride ion and water molecule forms a different number of contacts with the surrounding methylene hydrogens, as summarized in Table 5.

Table 5. Intermolecular contacts with chloride hydrate Cl and O atoms in **2**.H_2O.

Atom	Number of contacts	Distance range
Cl1	4	2.6 – 3.0 Å
Cl2	3	2.6 – 3.0 Å
O1	0	2.3 – 2.6 Å
O2	3	2.3 – 2.6 Å

Proton donor interactions to chloride reduce the ability of chloride to act as a proton acceptor (lengthens the hydrogen bond), whereas proton donor interactions to water increases the ability of water to act as a proton donor (shortens the hydrogen bond). The big difference between O1 and O2 means that the

chloride hydrogen bonds to O2 are the shortest. These principles explain the trends in Cl---O distances reported in Table 6.

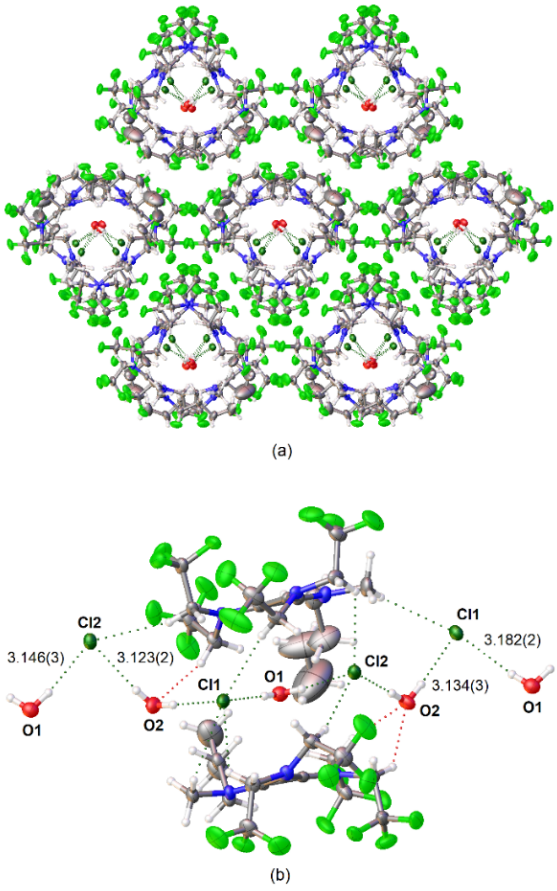

Figure 6. (a) Packing arrangement of the channels in **2**.H_2O; (b) intermolecular interactions between the cations and the polymer chain (distances in Å).

Table 6. Selected structural parameters that characterize hydrogen bonding interactions within the chloride hydrate polymer of **2**.H_2O.

Distance		Angle	
Cl1---O1	3.182(2) Å	Cl1-O1-Cl2	94.17(6)°
Cl2---O1	3.146(3) Å	Cl1-O2-Cl2	110.5(6)°
Cl1---O2	3.134(3) Å	O1-Cl1-O2	86.86(6)°
Cl2---O2	3.123(2) Å	O1-Cl2-O2	88.42(6)°

From Table 6, it is also apparent that the Cl-O-Cl angles at O1 and O2 are quite different but both are greater than 90°, whereas the O-Cl-O angles at Cl1 and Cl2 are quite similar and slightly less than 90°.

These are quite similar to structural parameters reported by Suresh and co-workers, who described a hydrogen-bonded one dimensional hybrid water-chloride motif in which a 1D polymer of $\{[Cl(H_2O)]^-\}_\infty$ is hydrogen-bonded to the cation via OH–chloride hydrogen bonds (Figure 7).[27] The packing of the cation and the hydrogen bonding from the OH group is likely to dictate the spacing between the chloride ions. The O–Cl distances are 3.184(4) and 3.093(4) Å while both the Cl-O-Cl and O-Cl-O angles (as dictated by symmetry) are 95.82(9)°. The average of the corresponding angles in **2**.H_2O is 95.0°. None of these structural parameters then are particularly dissimilar from the structural parameters in **2**.H_2O which is probably because the Cl^-–Cl^- distances are similar (4.6581(10) Å versus 4.6343(10) Å and 5.1413(10) Å in **2**.H_2O). Rotation about the Cl-O-Cl-O dihedral angles is expected to be facile, and so this is where we would expect the greatest structural differences. In this polymer the dihedral angles are 180° whereas in **2**.H_2O they vary from –115.70(5)° to 169.60(5)° (Table 2).

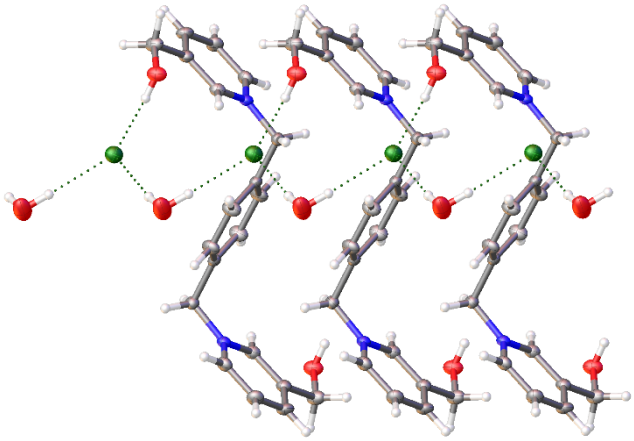

Figure 7. A non-discrete one-dimensional chain of $\{[Cl(H_2O)]^-\}_\infty$.[27]

Computational analysis

According to quantum chemical calculations, dichloride monohydrate is unstable in the gas phase (dissociating to form a stable chloride monohydrate plus a separate chloride ion) and dichloride dihydrate is metastable (two chloride monohydrates are more stable but the dichloride dihydrate represents a local minimum on the global potential energy surface), whereas dichloride tri- and tetra-hydrates all form stable complexes that represent global minima on their respective potential energy surfaces.[4,7,8,20] Therefore, both the tetrachloride tetrahydrate and chloride hydrate polymer are expected to be unstable in the gas phase, losing chlorides to form sub-stoichiometric $[Cl_{n-i}(H_2O)_n]^{(n-i)-}$ complexes, where *n* represents the initial number of chloride ions and water molecules, and *i* the number of chlorides lost before a stable gas phase complex can be formed. This means that it is not straightforward to compute and compare gas phase predictions of structures and/or vibrational spectra with condensed phase experimental measurements to establish how environmental effects contribute to stabilizing the chloride hydrates. Clearly, for both structures presented here, crystal packing effects are responsible for confining the chloride ions and water molecules within channels and voids created by surrounding cyclopropenium cations, enabling chloride hydrate oligomers and polymers to form. However, there do not appear to be any specific intermolecular interactions that particularly stabilize or template the chloride hydrates.

To disentangle the relative importance of crystal packing effects vs specific stabilization interactions on the structure and bonding within encapsulated chloride hydrates, a geometry optimization was performed at B3LYP/6-31+G(d,p) on the tetrachloride tetrahydrate from **1**.H_2O keeping the chloride ion positions fixed, followed by a partial Hessian harmonic frequency calculation to obtain a predicted IR spectrum. The importance of dispersion corrections was investigated using B3LYP-D3 models, which yielded structures and vibrational frequencies in very close

agreement to those obtained using B3LYP (Table 7S). The results are far more sensitive to basis set incompleteness; dropping polarization functions from the hydrogen atoms has a much larger effect on predicted transition frequencies. Not fixing the chloride positions leads to a variety of sub-stoichiometric $[Cl_{n-i}(H_2O)_n]^{(n-i)-}$ complexes during geometry optimization, so no attempts were made to compute vibrational frequencies without positional constraints on the chloride ions.

The optimized structure was found to be C_{2h} symmetric with the terminal waters on opposite sides of the square plane (see Figure 4). Although this is quite different to the tetrachloride tetrahydrate geometry within the crystalline environment, the out-of-plane angle that controls the orientation of the terminal water molecules is expected to be quite soft due to the relatively weak intermolecular interactions formed between the tetrachloride tetrahydrate and the surrounding cyclopropenium ions, and so this is not expected to particularly influence the positions of IR band centres for covalent bending and stretching modes.

Unfortunately, this same analysis cannot be applied to the chloride hydrate polymer from **2**.H_2O because it completely rearranges upon geometry optimization in the gas phase, even if chloride ion positions are kept fixed. Therefore, IR spectra were simulated within the crystalline environment using condensed-phase DFTB models (GFN1-xTB and SCC-DFTB-D3). The same calculations were also performed on the tetrachloride tetrahydrate for benchmarking purposes.

Table 7. Experimental and calculated anharmonic vibrational frequencies (in cm^{-1}) for **1**.H_2O and **1**.D_2O.

Solid-state experimental[a]	Gas phase calculated[b]	GFN1-xTB (gas)	GFN1-xTB (crystal)	SCC-DFTB-D3 (gas)	SCC-DFTB-D3 (crystal)	Deuterated experimental[a]	Assignment
3487 m	3484	3563	3575	3596	3675	2594 m	v(asym, inner)[c]
3418 s	3472	3526	3496	3565	3616	2517 s	v(asym, outer)[c]
3418 s	3416	3454	3487	3331	3404	2517 s	v(sym, inner)
3357 ms,sh	3389	3410	3423	3319	3373	2470 ms	v(sym, outer)
3263 w	3312, 3294	3025, 2997	2937, 2927	3119, 3093	3061, 3044	2396 w	2v(bend, outer/inner)
1641 m	1656, 1647	1512, 1499	1468, 1463	1560, 1547	1530, 1522	Not observed	v(bend, outer/inner)

[a] s = strong intensity; ms = medium-strong; m = medium; w = weak; sh = shoulder.
[b] Frequencies computed at B3LYP/6-31+G(d,p) with an empirical anharmonic correction applied; $\nu_{anh} = \nu_{harm} - 0.00001215\ \nu_{harm}^2$.
[c] These modes predicted to mix according to B3LYP and SCC-DFTB-D3 models and invert according to GFN1-xTB.

Infrared spectroscopy

Vibrational spectroscopy provides fundamental information about the bonding within these chloride hydrate structures.[28] The absence of any other O–H or N–H bonds makes these species ideal for study by infrared spectroscopy. Mid-IR spectra were recorded for **1**.H_2O and **2**.H_2O as well as the deuterated isotopomers **1**.D_2O and **2**.D_2O, both of which contain some residual H.

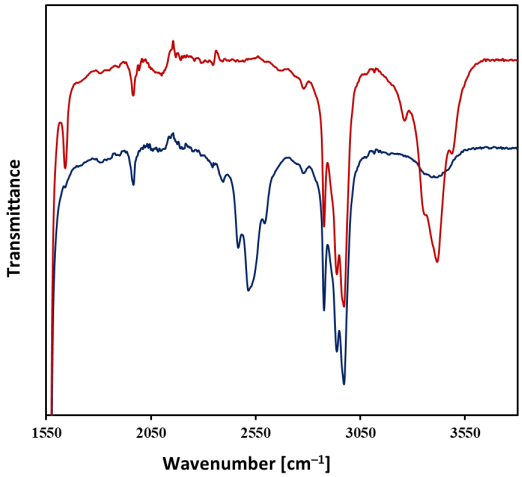

Figure 8. FT-IR spectra of **1**.H_2O (top) and **1**.D_2O (bottom).

Figure 8 shows the spectra for the hydrates of **1** and the vibrational modes are provided in Table 7. The C_i symmetry of the tetrameric cluster leads to four infrared-active fundamental stretching vibrations. The slightly distorted shape of the strong

band at 3418 cm^{-1} suggests that this is two overlapping bands. Comparison of its spectrum with the related tetrahydrate $[Cl_2(H_2O)_4]^{2-}$ is not especially useful in this case because that tetrahydrate contains one water with a very weak hydrogen bond which gives a high energy band at 3632 cm^{-1}, thus not affecting the rest of the bands to the same extent. A better way to look at the spectrum is as a combination of a C_{2h}-symmetric dichloride dihydrate core, $[Cl_2(H_2O)_2]^{2-}$, from $[C_3(N(CH_2CF_3)_2)(NBu_2)_2]Cl.H_2O$ and a dichloride monohydrate termini, $[Cl_2(H_2O)]^{2-}$, from $[C_3(N(CH_2CF_3)_2)_2(NHex_2)]Cl{\cdot}0.5H_2O$.

The reference $[Cl_2(H_2O)_2]^{2-}$ cluster has slightly shorter Cl–O distances of 3.2568(18) and 3.2182(15) Å than the dichloride dihydrate core in **1**.H_2O, so its IR bands at 3444 and 3392 cm^{-1} would be expected to be at lower wavenumbers than in **1**.H_2O. This helps us assign the bands at 3487 and around 3418 cm^{-1} as the ring vibrational modes ν(asym, inner) and ν(sym, inner), respectively, of the square (Figure 9).

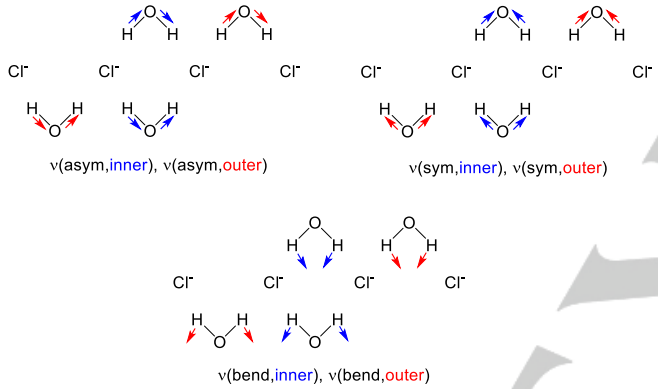

Figure 9. IR-active vibrational modes of $[Cl_4(H_2O)_4]^{4-}$.

As noted earlier, the $[Cl_2(H_2O)]^{2-}$ cluster has longer Cl–O distances than in **1**.H_2O, so its IR bands should be at higher energy than in **1**.H_2O; they appear at 3461 and 3408 cm^{-1} in the monohydrate, so the bands near 3418 and at 3357 cm^{-1} can be assigned to vibrational modes of the outer waters, ν(asym, outer) and ν(sym, outer), respectively.

These assignments are consistent with computational predictions (Table 7 and Figure 9), although both B3LYP and SCC-DFTB-D3 predict mixing between the inner and outer asymmetric stretching modes, while GFN1-xTB predicts the outer asymmetric stretch to occur at higher wavenumbers than the corresponding ring mode. B3LYP transition frequencies align semi-quantitatively with experimental band centres, while DFTB models yield assignments that are only qualitatively correct, regardless of whether the chloride hydrate is modelled in the gas phase or *in crystallo*.

For bending modes, DFTB computational method errors far outweigh crystal packing effects; and correcting for crystal packing effects only moves DFTB values further from experiment. Gas-phase B3LYP calculations, on the other hand, yield bending fundamentals in good agreement with experiment, with bending overtones in slightly worse agreement due to additional anharmonicity that is not accounted for by the anharmonicity correction parameterized for fundamentals. Although two bending fundamentals are predicted, their transition wavenumbers are so close that only a single band centre can be resolved experimentally.

Table 8. Experimental and calculated vibrational frequencies (in cm^{-1}) for **2**.H_2O and **2**.D_2O.

Solid-state experimental[a]	GFN1-xTB	SCC-DFTB-D3	Deuterated experimental[a]	Assignment
3347 s	3472/3458	3594/3559	2502 s	ν(asym)
3285 m	3404/3387	3354/3321	2468 m	ν(sym)
3258 w,sh			2446 w,sh	2ν(bend)
1658 w	1474	1535		ν(bend,even)
1646 vw	1462	1527		ν(bend,odd)

[a] s = strong; m = medium; w = weak; vw = very weak; sh = shoulder.

The IR spectrum of **2**.H_2O and **2**.D_2O is shown in Figure 10 and its vibrational modes are tabulated and assigned in Table 8. As mentioned earlier, the Cl–O distances in **2**.H_2O are shorter than found in the other discrete chloride hydrates. This would be expected to result in lower energy O–H stretching bands and, indeed, that is the case; the highest-energy, and most intense, band occurs at 3347 cm^{-1} for **2**.H_2O and this is associated with asymmetric stretches of the polymer waters. A significantly weaker band that appears at 3285 cm^{-1} is assigned to symmetric stretches of the polymer waters while a weak shoulder at 3258 cm^{-1} is assigned as an overtone of the bending vibrations. Like the stretching modes, the bending region has two bands: a more intense one at higher energy (1658 cm^{-1}) and a less intense band at lower energy (1646 cm^{-1}). Condensed phase DFTB calculations predict four stretching bands and two bending bands; corresponding to in-phase bending and symmetric/asymmetric stretching modes of alternate water molecules within the polymer chain (Figure 11). However, because these water molecules are in similar environments, the differences in stretching fundamentals are small and cannot be resolved experimentally (Table 8). While the differences in bending fundamentals are also small, the sharpness of the bending bands within the experimental spectrum means that these can be resolved.

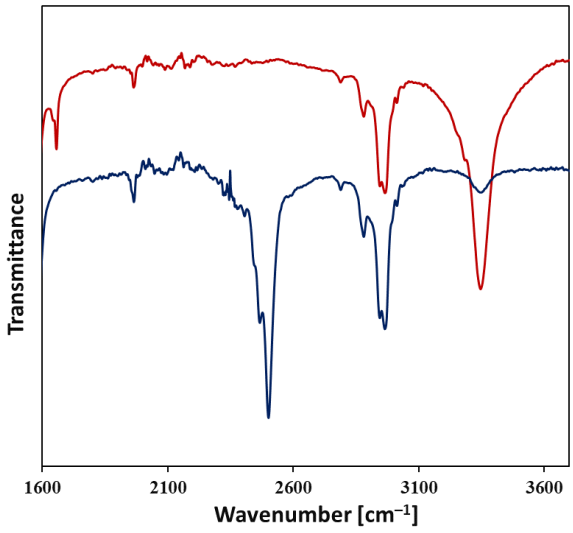

Figure 10. FT-IR spectra of **2**.H_2O (top) and **2**.D_2O (bottom).

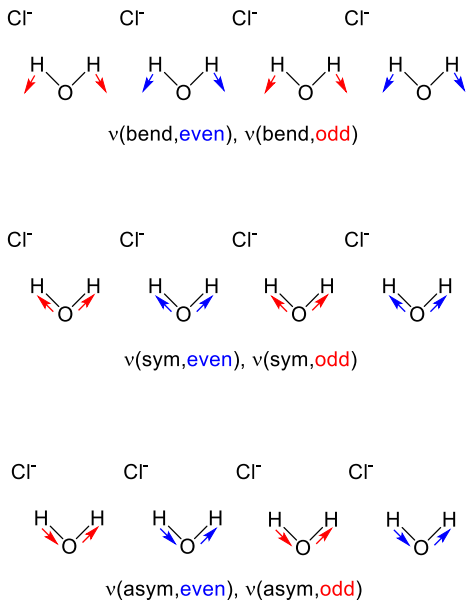

Figure 11. IR-active vibrational modes of $\{[Cl(H_2O)]^-\}_\infty$.

Conclusions

Although the monochloride monohydrate is the most thermodynamically-stable structure for $[Cl(H_2O)]^-$, the dimeric structure is calculated to be stable in the gas phase as a metastable species and has also been frequently observed in the solid state. We have now shown that it is possible to isolate tetrameric and polymeric structures of $[Cl(H_2O)]^-$ with the isolation of $[Cl_4(H_2O)_4]^{4-}$ and a one-dimensional linear polymeric chain of $\{[Cl(H_2O)]^-\}_\infty$. The tetramer is structurally very similar to the known discrete dichloride tetrahydrate and monohydrate, but spectroscopically it is more similar to the dichloride dihydrate and monohydrate, based upon comparisons to previously published experimental data for these species, along with *ab initio* gas phase predictions. This is consistent with what we would describe as a "discrete" cluster. We also benchmarked condensed-phase plane-wave DFTB models for the tetramer both in the gas phase (with constrained chloride ion positions) and *in crystallo*, and showed that these models are far less accurate for predicting vibrational frequencies than their Kohn-Sham orbital based DFT counterparts. They can only be used to obtain qualitative spectral assignments.

The polymeric structure forms within a relatively hydrophilic environment, with the fluorinated chains on the outside of the chloride hydrate channels. The Cl–O distances in the polymer are consistent with only weak interactions with the environment while the angles at Cl are near 90° which possibly also indicates that the interactions with the environment are weak. Condensed-phase DFTB models were used to investigate and assign the infrared spectra of the polymer. Oligomeric and polymeric structures of $[Cl(H_2O)]^-$ are computationally unstable in the gas phase, but this study shows that encapsulation of such species in a suitable environment allows for their formation. It also indicates that the use of gas phase studies to investigate the speciation of anion solvates has its limits in terms of what species it can predict as being isolable. It would be reasonable to expect that other discrete oligomeric chloride hydrates could be isolated.

The combination of a triaminocyclopropenium cation that has very weak cation-anion interactions, coupled with the hydrophobic environment provided by fluorinated alkyl substituents that both limits the amount of water present while also concentrating the chloride hydrate into the more hydrophilic methylene regions, favours the formation of these oligomeric and polymeric structures.

Experimental Section

All the experimental work and sample preparation were carried out under dried nitrogen atmosphere using standard Schlenk techniques. CH_2Cl_2, diethylether, acetone, $CHCl_3$, CH_3OH, D_2O, silica, triethylamine, tributylamine, dipropylamine, butylmethylamine and $NH(CH_2CF_3)_2$ were obtained commercially. C_3Cl_4 was prepared according to a literature procedure.[29,30] Solvents were dried using an in-house solvent purification system.

^1H-, $^{13}C\{^1H\}$- and ^{19}F-NMR spectra were collected on an JEOL ECZ400S spectrometer operating at 400, 100 and 376 MHz, respectively, referenced to residual solvent peaks. Mid-IR data were collected at room temperature by using a Vertex 70 FT-IR spectrometer from Bruker (Germany), operating with a Platinum ATR unit with a diamond crystal. A resolution of 4 cm^{-1} and 16 scans were taken. Electrospray mass spectrometry was carried out on a Micromass LCT, with samples dissolved in acetonitrile. Microanalyses were performed by Campbell Microanalytical Laboratory, University of Otago, Dunedin.

(Diethylamino)(dipropylamino)(bis(2,2,2-trifluoroethyl)amino)cyclopropenium chloride, $[C_3(N(CH_2CF_3)_2)(NEt_2)(NPr_2)]Cl.H_2O$

NEt_3 (1.819 g, 17.79 mmol) and $NH(CH_2CF_3)_2$ (8.004 g, 42.23 mmol) were dissolved in CH_2Cl_2 (10 mL) and added slowly to C_3Cl_4 (1.81 g, 10.2 mmol) in CH_2Cl_2 (30 mL) at 0 °C with stirring. Stirring was continued for 5 h. A mixture of $NHPr_2$ (0.867 g, 8.48 mmol) and NEt_3 (0.863 g, 8.44 mmol) in CH_2Cl_2 (5 mL) was added at 0 °C and stirring continued at 0 °C for 4 h and then at ambient temperature for 48 h. CH_2Cl_2 was removed *in vacuo* and acetone (100 mL) was added to the mixture. A precipitate was filtered off and acetone was removed *in vacuo*. Water (100 mL) was added and then washed with diethylether (10 × 30 mL). The aqueous layer was extracted with $CHCl_3$ (6 × 30 mL). $CHCl_3$ was removed *in vacuo* and chromatographic (silica) separation (elution was done with CH_2Cl_2 and slowly increasing amounts of methanol) yielded a pale yellow product (0.7 g, 16%). Crystallographic quality crystals of the monohydrate were obtained by evaporation of an undried CH_2Cl_2/diethylether solution. ^1H NMR (CD_3OD, 400 MHz): 4.35 (q, $^3J_{HH}$ = 8.7 Hz, 4H, NCH_2CF_3), 3.51 (t, $^3J_{HH}$ = 7.3 Hz, 4H, NCH_2CH_3), 3.40 (t, $^3J_{HH}$ = 7.8 Hz, 4H, NCH_2CH_2), 1.72 (m, 4H, $NCH_2CH_2CH_3$), 1.31 (t, $^3J_{HH}$ = 7.2 Hz, 6H, CH_2CH_3), 0.97 (t, $^3J_{HH}$ = 7.4 Hz, 6H, CH_3). $^{13}C\{H\}$ NMR (CD_3OD, 100 MHz): 125.72 (q, $^1J_{CF}$ = 280.3 Hz, NCH_2CF_3), 121.30 (C_3 NCH_2CF_3), 120.93 (C_3 NCH_2CH_3), 114.69 (C_3 $NCH_2CH_2CH_3$), 55.71 ($NCH_2CH_2CH_3$), 55.55 (q, $^2J_{CF}$ = 33.7 Hz NCH_2CF_3), 48.40 (NCH_2CH_3), 22.83 ($NCH_2CH_2CH_3$), 14.07 (NCH_2CH_3), 11.05 ($NCH_2CH_2CH_3$). ^{19}F NMR (CD_3OD, 376 MHz): –72.63 (t, $^3J_{HF}$ = 8.7 Hz, NCH_2CF_3), ES^+ m/z 388.2178 (100%, M^+). Calculated for $C_{17}H_{28}F_6N_3^+$ (ES^+) m/z 388.2182. $C_{17}H_{28}F_6N_3Cl.H_2O$: C, 46.21; H, 6.84; N, 9.51; Found: C, 46.09; H, 6.67; N, 8.88. A deuterated sample was prepared by addition of a few drops of D_2O to a CH_2Cl_2 solution followed by removal of solvent *in vacuo*. This was repeated until the desired level of deuteration was achieved.

(Butylmethylamino)bis(bis(2,2,2-trifluoroethyl)amino) cyclopropenium chloride, $[C_3(N(CH_2CF_3)_2)_2(NBuMe)]Cl$

NBu_3 (4.74 g, 25.3 mmol) and $NH(CH_2CF_3)_2$ (12.04 g, 63.51 mmol) were dissolved in CH_2Cl_2 (10 mL) and added slowly to C_3Cl_4 (2.71 g, 15.2 mmol) in CH_2Cl_2 (40 mL) at 0 °C with stirring. The stirring was continued for 2 h. A mixture of NHBuMe (1.126 g, 12.53 mmol) and NBu_3 (2.3 g, 12.28 mmol) in CH_2Cl_2 (5 mL) was added to the mixture at 0 °C and stirring continued at 0 °C for 4 h and then at ambient temperature for 48 h. CH_2Cl_2 was removed *in vacuo* and the residue was dissolved in deionized water (150 mL) and extracted with diethylether (4 × 50 mL). The volume of diethylether was reduced *in vacuo* to 50 mL and the product extracted with deionized water (6 × 50 mL). Water was removed *in vacuo*. This mixture was separated through a silica column by a gradual elution method using CH_2Cl_2 and increasing amounts of ethanol. Removal of ethanol gave a white powder (1.2 g, 15%). Crystallographic quality crystals of the monohydrate were obtained by evaporation of an undried EtOH/diethylether solution. ^{1}H NMR (CD_3CN, 400 MHz): 4.31 (q, $^3J_{HF}$ = 8.2 Hz, 8H, NCH_2CF_3), 3.37 (t, $^3J_{HH}$ = 7.8 Hz, 2H, NCH_2), 3.15 (s, 3H, NCH_3), 1.63 (m, 2H, NCH_2CH_2), 1.32 (m, 2H, $NCH_2CH_2CH_2$), 0.93 (t, $^3J_{HH}$ = 7.3 Hz, 3H, CH_3). $^{13}C\{^1H\}$ NMR (CD_3OD, 100 MHz): 125.51 (q, $^1J_{CF}$ = 280.3 Hz, CH_2CF_3), 124.47 (C_3 NCH_2CF_3), 57.66 (NCH_3), 55.74 (q, $^2J_{CF}$ = 34.7 Hz, NCH_2CF_3), 40.83 (NCH_2), 30.55 (NCH_2CH_2), 20.64 ($NCH_2CH_2CH_2$), 14.13 (CH_3). ^{19}F NMR (CD_3CN, 376 MHz): –71.60 (broad s, NCH_2CF_3), ES^+ m/z 482.1460 (100%, M^+); calculated for $C_{16}H_{20}F_{12}N_3^+$ 482.1460. Microanalysis: Exptl. C, 35.92; H, 4.34; N, 7.53%. Calc. for $C_{16}H_{20}N_3ClF_{12}.H_2O$: C, 35.87; H, 4.14; N, 7.84%. A deuterated sample was prepared by addition of a few drops of D_2O to a CH_2Cl_2 solution followed by removal of solvent *in vacuo*. This was repeated until the desired level of deuteration was achieved.

Crystal data

Suitable crystals were mounted on a SuperNova, Dual, Mo at zero, Atlas diffractometer. Using Olex2,[31] the structure was solved with the XT structure solution program[32] and refined with the XL refinement package[32] using Least Squares minimisation with anisotropic thermal parameters for all non-hydrogen atoms. Hydrogen atoms on the methylene groups were refined isotropically at their calculated positions and methyl groups were refined as rotating groups. The water protons were located from the density difference map and refined isotropically. CCDC 2058695 and 2058696 contain the supplementary crystallographic data for **2**.H_2O and **1**.H_2O, respectively. This data can be obtained free of charge from The Cambridge Crystallographic Data Centre.

Computational

Constrained geometry optimizations and harmonic vibrational frequency calculations were performed on gas-phase $[Cl_4(H_2O)_4]^{4-}$ clusters at B3LYP/6-31+G* using the QChem5.0 program package.[33] Initial atomic positions were derived from the crystal structure, and chloride atom positions kept fixed throughout the geometry optimization process. A partial Hessian calculation was carried out,[34–36] allowing only the water molecules to vibrate and all resultant harmonic frequencies were real, confirming that it represents a minimum on the potential energy surface subject to the applied constraints. An empirical quadratic correction model was applied to obtain predicted anharmonic vibrational frequencies:[37]

$$\nu_{anh} = \nu_{harm} - 0.00001215\ \nu_{harm}^2$$

Similar gas phase calculations were performed using the GFN1-xTB[38] and SCC-DFTB-D3[39] models as implemented within the DFTB module of the Amsterdam Modelling Suite.[40] These DFTB models were chosen because they have been specifically parameterised and benchmarked for accurately predicting vibrational frequencies.[38,39]

Plane-wave DFTB calculations were performed on infinitely periodic crystalline **1**.H_2O and **2**.H_2O, also using the GFN1-xTB[38] and SCC-DFTB-D3[39] models as implemented within the DFTB module of the Amsterdam Modelling Suite.[40] The cyclopropenium molecules were constrained to remain at their crystallographically determined positions, while the positions of all atoms within the chloride hydrates were optimized. This was followed by partial Hessian calculations involving only the chloride atoms and water molecules. All predicted vibrational frequencies were real, confirming that the chloride ions and water molecules had fully optimized to a minimum energy conformation, subject to the applied constraints on the positions of the cyclopropenium atoms.

Acknowledgements

Dr. Matthew I. J. Polson (University of Canterbury) is thanked for his assistance with the X-ray crystallography.

Keywords: chloride • hydrate • infrared • solvate • X-ray diffraction

[1] M. S. Abdelbassit, O. J. Curnow, E. Libowitzky, R. O. Piltz, *J. Phys. Chem. A* **2020**, *124*, 9244-9251.

[2] a) P. Bajaj, D. Zhuang, F. Paesani, *J. Phys. Chem. Lett*. **2019**, *10*, 2823-2828; b) G. M. Chaban, J. O. Jung, R. B. Gerber, *J. Phys. Chem. A*. **2000**, *104*, 2772-2779; c) J.-H. Choi, K. T. Kuwata, Y.-B. Cao, M. Okumura, *J. Phys. Chem. A*. **1998**, *102*, 503-507; d) E. G. Diken, J. M. Headrick, J. R. Roscioli, J. C. Bopp, M. A. Johnson, A. B. McCoy, X. Huang, S. Carter, J. M. Bowman, *J. Phys. Chem. A*. **2005**, *109*, 571-575; e) H. E. Dorsett, R. O. Watts, S. S. Xantheas, *J. Phys. Chem. A*. **1999**, *103*, 3351-3355; f) J. Kim, H. M. Lee, S. B. Suh, D. Majumdar, K. S. Kim, *J. Chem. Phys*. **2000**, *113*, 5259-5272; g) W. Punyain, K. Takahashi, *Phys. Chem. Chem. Phys*. **2016**, *18*, 26970-26979; h) J. Rheinecker, J. M. Bowman, *J. Chem. Phys*. **2006**, *125*, 133206; i) W. H. Robertson, M. A. Johnson, *Annu. Rev. Phys. Chem*. **2003**, *54*, 173-213; j) J. R. Roscioli, E. G. Diken, M. A. Johnson, S. Horvath, A. B. McCoy, *J. Phys. Chem. A*. **2006**, *110*, 4943-4952; k) X.-G. Wang, T. Carrington Jr, *J. Chem. Phys*. **2014**, *140*, 204306; l) S. S. Xantheas, *J. Phys. Chem.* **1996**, *100*, 9703-9713; m) H. Zhao, D. Xie, H. Guo, *J. Chem. Phys*. **2018**, *148*, 064305.

[3] a) P. Ayotte, S. B. Nielsen, G. H. Weddle, M. A. Johnson, S. S. Xantheas, *J. Phys. Chem. A*. **1999**, *103*, 10665-10669; b) S. Horvath, A. B. McCoy, B. M. Elliott, G. H. Weddle, J. R. Roscioli, M. A. Johnson, *J. Phys. Chem. A*. **2009**, *114*, 1556-1568.

[4] O. J. Curnow, R. G. Maclagan, *ChemPhysChem*. **2012**, *13*, 3271-3274.

[5] E. J. MacLean, R. I. Robinson, S. J. Teat, C. Wilson, S. Woodward, *J. Chem. Soc., Dalton Trans*. **2002**, 3518.

[6] J. G. Małecki, R. Kruszynski, Z. Mazurak, *Polyhedron* **2009**, 28, 3891.

[7] C. H. Choi, S. Re, M. H. O. Rashid, H. Li, M. Feig, Y. Sugita, *J. Phys. Chem. B* **2013**, *117*, 9273.

[8] A. S. Ivanov, G. Frenking, A. I. Boldyrev, *J. Phys. Chem. A*. **2014**, *118*, 7375-7384.

[9] R. Senthooran, O. J. Curnow, T. Brenner, R. Weiss, M. Ferreras, D. L. Crittenden, *ChemPlusChem* **2020**, *85*, 2272-2280.

[10] A. J. Wallace, C. D. Jayasinghe, M. I. Polson, O. J. Curnow, D. L. Crittenden, *J. Am. Chem. Soc*. **2015**, *137*, 15528-15532.

[11] a) R. Weiss, T. Brenner, F. Hampel, A. Wolski, *Angew. Chem. Int. Ed. Engl*. **1995**, *34*, 439; b) R. Weiss, M. Rechinger, F. Hampel, A. Wolski, *Angew. Chem. Int. Ed. Engl*. **1995**, *34*, 441; c) R. Weiss, O. Schwab, F. Hampel, *Chem. Eur. J*. **1999**, *5*, 968 d) R. Weiss, K. Schloter, *Tetrahedron Lett*. **1975**, *40*, 3491.

[12] D.-X. Wang, S.-X. Fa, Y. Liu, B.-Y. Hou, M.-X. Wang, *Chem. Commun.* **2012**, *48*, 11458-11460.

[13] E. F. Kleinman, J. Bordner, B. J. Newhouse, K. MacFerrin, *J. Am. Chem. Soc.* **1992**, *114*, 4945–4946.

[14] A. Basu, G. Das, *Chem. Commun.* **2013**, *49*, 3997-3999.

[15] A. Szumna, J. Jurczak, *Helv. Chim. Acta*. **2001**, *84*, 3760-3765.

[16] D. A. Safin, M. G. Babashkina, K. Robeyns, Y. Garcia, *New J. Chem.* **2017**, *41*, 8263-8269.

[17] a) J. R. Butchard, O. J. Curnow, D. J. Garrett, R. G. Maclagan, *Angew. Chem*. **2006**, *45*, 7550-7553; b) J. R. Butchard, O. J. Curnow, D. J. Garrett, R. G. Maclagan, E. Libowitzky, P. M. Piccoli, A. J. Schultz, *Dalton Trans*. **2012**, *41*, 11765-11775.

[18] M. S. Abdelbassit, O. J. Curnow, M. Ferreras, D. L. Crittenden, *ChemPlusChem* **2020**, *85*, 927-932.

[19] O. J. Curnow, R. Senthooran, *Dalton Trans.* **2020**, *49*, 9579-9582.

[20] a) A. Galashev, F. Sigon, A. Servida, *J Struct Chem*. **1996**, *37*, 252-259; b) J. Gao, S. Boudon, G. Wipff, *J. Am. Chem. Soc*. **1991**, *113*, 9610-9614;

[21] F. F. Jian E. Liu, J. Ma, *Supramolecular Chemistry* **2018**, *30*, 960-964.

[22] S. K. Seth, *Inorg. Chem. Commun*. **2014**, *43*, 60-63.

[23] H. Y. Wang, H. Y. Liu, *Transit. Met. Chem*. **2017**, *42*, 165-173.

[24] S. S. Bhat, V. K. Revankar, A. Khan, R. J. Butcher, K. Thatipamula, *New J. Chem.* **2015**, *39*, 3646-3657; D. L. Reger, R. F. Semeniuc, C. Pettinari, F. Luna-Giles, M. D. Smith, *Cryst. Growth Des*. **2006**, *6*, 1068; W. Liu, W. Xu, J.-L. Lin, H.-Z. Xie, *Acta Cryst*. **2008**, *E64*, m1586; R. R. Fernandes, A. M. Kirillov, M. F. C. Guedes da Silva, Z. Ma, J. A. L. da Silva, J. J. R. Fraústo da Silva, A. J. L. Pombeiro, *Cryst. Growth Des*. **2008**, *8*, 782; S. K. Padhi, R. Sahu, V. Manivannan, *Polyhedron* **2010**, *29*, 709-714; E. C. Constable, J. Lewis, M. C. Liptrot, P. R. Raithby, *Inorg. Chim. Acta* **1990**, *178*, 47; B. N. Figgis, E. S. Kucharski, A. H. White, *Aus. J. Chem*. **1983**, *36*, 1563; P. Paul, B. Tyagi, A. K. Bilakhiya, M. M. Bhadbhade, E. Suresh, *J. Chem. Soc., Dalton Trans*. **1999**, 2009; E. C. Constable, S. M. Elder, D. A. Tocher, *Polyhedron* **1992**, *11*, 1337; S. S. Bhat, V. K. Revankar, *J. Chem. Cryst*. **2016**, *46*, 9-14.

[25] P. C. Junk, C. J. Kepert, L. I. Semenova, B. W. Skelton, A. H. White, *Z. Anorg. Allg. Chem*. **2006**, *632*, 1293; R. E. Rulke, V. E. Kaasjager, D. Kliphuis, C. J. Elsevier, P. W. N. M. van Leeuwen, K. Vrieze, K. Goubitz, *Organometallics* **1996**, *15*, 668; C. S. Angle, A. G. DiPasquale, A. L. Rheingold, L. H. Doerrer, *Acta Cryst. C* **2006**, *62*, m340.

[26] H. B. Friedrich, G. E. M. Maguire, B. S. Martincigh, M. G. McKay, L. K. Pietersen, *Acta Cryst. E* **2008**, *64*, m1240.

[27] K. K. Bisht, A. C. Kathalikkattil, E. Suresh, *Cryst. Growth Des.* **2012**, *12*, 556-561.

[28] N. C. Polfer, J. Oomens, *Mass Spectrom. Rev.* **2009**, *28*, 468-494.

[29] M. A. Bell, MSc thesis, Georgia Institute of Technology (USA), **1968**.

[30] S. W. Tobey, R. West, *Tetrahedron Lett.* **1963**, *4*, 1179-1182.

[31] O. V. Dolomanov, L. J. Bourhis, R. J. Gildea, J. A. K. Howard, H. Puschmann, *J. Appl. Cryst*. **2009**, *42*, 339-341.

[32] G. M. Sheldrick, *Acta Cryst*. **2008**, *A64*, 112-122.

[33] Y. Shao, Z. Gan, E. Epifanovsky, A. T. Gilbert, M. Wormit, J. Kussmann, *et al*., *Mol. Phys*. **2015**, *113*, 184-215.

[34] J. D. Head, *Int. J. Quant. Chem*. **1997**, *65*, 827-838.

[35] A. Ghysels, D. van Neck, V. van Speybroeck, T. Verstraelen, M. Waroquier, *J. Chem. Phys*. **2007**, *126*, 224102.

[36] N. A. Besley, J. A. Bryan, *J. Phys. Chem. C* **2008**, *112*, 4308-4314.

[37] M. Sibaev, D. L. Crittenden, *J. Phys. Chem. A* **2015**, *119*, 13107-13112.

[38] S. Grimme, C. Bannwarth, P. Shushkov, *J. Chem. Theo. Comput*. **2017**, *13*, 1989-2009.

[39] H. A. Witek, K., Morokuma, *J. Comput. Chem*. **2004**, *25*, 1858-1864.

[40] G. T. Te Velde, F. M. Bickelhaupt, E. J. Baerends, C. Fonseca Guerra, S. J. van Gisbergen, J. G. Snijders, T. Ziegler, *J. Comput. Chem*. **2001**, *22*, 931-967.

Entry for the Table of Contents

A discrete tetramer and polymer of monochloride monohydrate

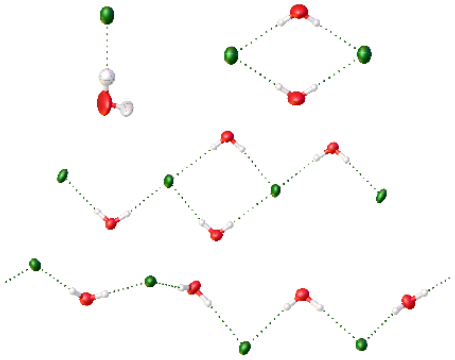

Rathiga Senthooran, Owen J. Curnow, and Deborah L. Crittenden**

The use of hydrophobic partially-fluorinated triaminocyclopropenium chloride salts provides a template for the formation of discrete chloride hydrate species. We have now isolated a discrete tetramer of chloride monohydrate, namely $[Cl_4(H_2O)_4]^{4-}$, as well as a polymeric analogue $\{[Cl(H_2O)]^-\}_\infty$. The structures and infrared spectra support the discrete nature of these species.

Page No. – Page No.

Discrete Oligomers and Polymers of Chloride Hydrate can form in Encapsulated Environments: Structures and Infrared Spectra of $[Cl_4(H_2O)_4]^{4-}$ and $\{[Cl(H_2O)]^-\}_\infty$